Winter Climatic Controls on Spring Snowpack Density in the Western United States

Winter Climatic Controls on Spring Snowpack Density in the Western United States

Bohumil M. Svoma*

*School of Geographical Sciences and Urban Planning, Arizona State University, P.O. Box 874601, Tempe, Arizona 85287-4601, U.S.A. Bohumil.Svoma@asu.edu

Abstract

For numerous climate studies, snowpack density is used to determine snow water equivalent from snow depth (or the reverse) or to determine snow surface albedo through the characterization of aging snow covers. In addition, high spring snowpack water content (and thus density) can act as a catalyst for wet avalanches. Surprisingly, there are few empirical studies that focus on spring snowpack density. In this study, spring snowpack densities in the western United States are statistically related to four variables that characterize the antecedent winter conditions: (1) mean air temperature for days without snowfall, (2) the fraction of precipitation falling as snow, (3) total precipitation, and (4) mean snowfall density. Areal composite regression analysis for the western United States indicates a highly significant ($p = 0.005$) positive relationship between winter precipitation total and April 1 snowpack density. This relationship weakens in lower elevation regions and coastal regions where warmer winter temperatures are conducive to more frequent rain events and melt events which affect snowpack density and ablate snow cover. These empirical results are supported by a simple snowpack model. The significant positive relationship between precipitation and density is likely due to increased densification rates through gravitational compaction from the presence of greater snow water equivalent resulting from more snowfall.

Introduction

An understanding of spring (April 1 in many snow investigations) snowpack density is of considerable importance for wet avalanche forecasting, climate modeling, and snow cover modeling. Wet avalanches occur due to the warming and melting of snowpacks with high water content (and therefore density) leading to less cohesion (Roeger et al., 2001). A modeling study by Lazar and Williams (2008) suggests a change toward an earlier occurrence of spring season wet avalanches in Colorado due to future warming. For many modeling and snow cover reconstruction studies, snow density is essential for determining snow depth, snow water equivalent, and surface albedo (e.g., Elder et al., 1998; Balk and Elder, 2000; Brown, 2000; Erxleben et al., 2002; Kelly et al., 2003; Brown et al., 2003; Garen and Marks, 2005; Flanner and Zender, 2006). For instance, Brown et al. (2003) used a simple snowpack model to generate large-scale snow cover information (including snowpack density) across North America for comparison to general circulation model snow cover output for the Atmospheric Model Intercomparison Project II. Mote et al. (2005) utilized the Variable Infiltration Capacity hydrologic model to supplement sparse measurements of snow water equivalent (SWE) in the western United States (U.S.A.), and Lazar and Williams (2008) used the Snow Thermal Model (SNTHERM) for determining increases in snowpack density due to regional warming under specific greenhouse gas emission scenarios.

From a theoretical standpoint, the processes influencing the densification of snow are well known (Kelly et al., 2003; Brown et al., 2003; Flanner and Zender, 2006). Various experimental studies have been conducted as well (as highlighted in a review by Colbeck (1982); Sturm and Benson, 1997; Kaempfer and Schneebeli, 2007).

The density of fresh snow or, snowfall density, is affected by ice crystal-structure which is impacted by in-cloud processes, sub-cloud level processes as the snow falls, and compaction at the surface due to various meteorological factors such as wind (Roebber et al., 2003). These mechanisms are extremely complex and not well understood (Roebber et al., 2003; Ware et al., 2006) but generally, warmer cloud temperatures and surface temperatures lead to denser snowfall (Bossolasco 1954; Diamond and Lowry, 1954; Hedstrom and Pomeroy, 1998; Judson and Doesken, 2000; Byun et al., 2008). In addition, compaction at the surface is influenced by precipitation rate, with higher precipitation rates leading to higher densities (Judson and Doesken, 2000; Byun et al., 2008). It has been found that during snowfall events with surface air temperature near 0 °C, the variation in air temperature is the most influential factor governing snowfall density while precipitation rate is the more dominant influence at colder temperatures (Byun et al., 2008). A more detailed discussion regarding snowfall density in terms of ice-crystal structure is beyond the scope of this paper. For a more in-depth discussion on cloud microphysical processes and snowfall density see Power et al. (1964) or Roebber et al. (2003).

After densification through surface compaction of fresh snowfall, the resulting snowpack continues to increase in density throughout the cold season. Compaction continues through the force of gravity mechanically rearranging the snow grains (Mizukami and Perica, 2008). Also, vapor pressure differences between concave and convex parts of snow grains cause "necks" to grow between snow particles and thus act to reduce the porosity of the snow, a process called sintering (Maeno and Ebinuma, 1983; Mizukami and Perica, 2008). In cold snowpacks, the snow grains themselves can continue to grow through vapor diffusion (Colbeck, 1982). These larger snow grains experience less sintering

than warmer snowpacks. In addition, warmer snowpacks that are isothermal at 0 °C or above experience snowmelt, and the liquid water is often retained in the snowpack or refreezes which in turn fills pore space and leads to snow densification (Mizukami and Perica, 2008). Similarly, rainfall over snowpacks can increase density (Brown et al., 2003); however, rainfall can also decrease density if the structure of the snowpack is reduced enough such that water can no longer be efficiently absorbed by the snow (Meloysund et al., 2007). Lastly, wind can affect snowpack density through compaction (Roeger et al., 2001; Meloysund et al., 2007) and through the loss of *SWE* through sublimation (Sturm et al., 2001). In simple snow cover models, the snowpack densification rate is often represented through empirical equations (Brown et al., 2003; Kelly et al., 2003). Generally, variables used in such equations include (1) precipitation total (or *SWE*), (2) precipitation type, (3) air temperature (for modeling snow melt), and (4) initial snowfall density.

Unfortunately, limited empirical research exists regarding the climatic controls on spring snowpack density (Mizukami and Perica, 2008). This is largely due to the lack of a long record of continuous data sites that measure snow depth (*SD*) and *SWE* of that depth, the variables needed to estimate snow density. Mizukami and Perica (2008) used SNOTEL sites in a seven year study of snowpack density in the western U.S.A. and found that snowpack density has less interannual variability than *SD* and *SWE*. Mizukami and Perica (2008) also found that, in mid March, snowpack densification rates increase across the entire west at nearly uniform rates and snowpack density characteristics are dependent on proximity to the Pacific Ocean and elevation, which is consistent with the findings of previous avalanche studies (Mock, 1995; Mock and Birkeland, 2000). It is important to note that Mizukami and Perica (2008) did not directly relate temperature and precipitation to density. In addition, due to the short periods of record of the SNOTEL data, only seven years were examined.

Localized studies (<100 km^2) concerned with modeling spring snowpack density for small high-elevation drainage basins in the west have also been conducted. Elder et al. (1998), Balk and Elder (2000), and Erxleben et al. (2002) spatially interpolated spring snowpack densities in the high elevations of the Sierra Nevada and Colorado Rocky Mountains based on regression equations with elevation, slope, aspect, and net solar radiation as independent variables. It is important to note that these studies were only concerned with interpolating snowpack density between measurement sites and therefore did not directly relate variables such as past precipitation and air temperature to snowpack density.

The purpose of this study is to establish the dominant densification mechanisms in the western U.S.A. through the analysis of data sets that largely contain more than 30 years of records. Spring snowpack densities are statistically related to four variables that characterize the meteorological conditions of the antecedent cold season. These four variables are well established in the literature (Brown et al., 2003; Kelly et al., 2003) as major influences on snow cover density and include (1) the ratio of snowfall to rainfall, (2) the average density of freshly fallen snow, (3) the average temperature of days with no snow accumulation, and (4) the total precipitation. Considering the relationship between snow cover density and abundant heavy snowfall due to the proximity to the Pacific Ocean (Mock, 1995; Mock and Birkeland, 2000; Mizukami and Perica, 2008), it is expected that total precipitation and snowfall density will be the more significant predictors of spring snowpack density.

Data

Snow course data for the 11 westernmost states in the contiguous U.S.A. (Fig. 1) were obtained from the U.S. Department of Agriculture National Resources Conservation Service (NRCS; downloaded from http://www.wcc.nrcs.usda.gov/snow/snowhist.html). These data consist of *SWE* and *SD* measured near the first of each month; however, data collected near April 1 were the focus of this study. This is the optimal date for analysis because it is the most frequent measurement date, and most locations throughout the west typically reach maximum *SWE* around this period (Mote et al., 2005). Snow courses are typically 300 m long and measurements are taken at multiple spots along this length in order to reduce the effects of snow drift (Pierce et al., 2008). Measurements of *SWE* are taken by driving a hollow tube into the snow and then determining the mass of the collected snow.

Additionally, daily precipitation, snowfall, and temperature data for the western U.S.A. were obtained from the National Weather Service Cooperative Observer (COOP) Network (Fig. 1; downloaded from http://www7.ncdc.noaa.gov/CDO/cdo). New snow is measured by trained observers either once every 24 hours, or from the sum of four sets of 6-hour observations with a goal of measuring the maximum accumulation over the 24-hour period (Baxter et al., 2005). Depth is measured by use of either a ruler or snow board. Multiple measurements are taken to determine a mean snow depth so the impacts of wind are minimized (Baxter et al., 2005). The liquid equivalent is measured by melting the contents collected in a precipitation gauge that is typically unshielded with a mouth diameter of 20 cm (Baxter et al., 2005; Pierce et al., 2008). If there is a noticeable discrepancy between the depth and liquid equivalent, the observer is instructed to take a core sample from the snow board (Baxter et al., 2005). In this study, the only COOP sites that were considered for analysis were those that were located within 50 m of elevation and 0.5° latitude and longitude from an NRCS snow course site (and *vice versa*; Fig. 1). Generally, the snow course data and COOP data used in this study had more than 30 years of records before quality control methods were applied. Lastly, as input for a simple snowpack model described in the methods below, 3-hourly North American Regional Reanalysis (NARR) 2 m air temperature and total accumulated precipitation were obtained from National Oceanic and Atmospheric Administration Earth Science Research Laboratory (http://www.esrl.noaa.gov/psd/data/gridded/data.narr.html). The grid resolution is approximately 0.3° and the data range from 1979 to 2009.

Methods

For each snow course, April 1 snowpack density (*SPD*) was calculated for each year. *SPD* is inversely related to the ratio of *SD* to *SWE* and is defined by the following equation (Mizukami and Perica, 2008):

$$\rho_s = \rho_w \frac{SWE}{SD} \qquad (1)$$

where ρ_s is the density of snow in kg m^{-3}, ρ_w is the density of liquid water (1000 kg m^{-3} at 0 °C), and *SWE* and *SD* are in the same units of depth. Snow courses with greater than 10% of April 1 observations with a snow depth of zero were discarded from the study.

The COOP data were culled in a method emulating Knowles et al. (2006), who worked with the Historical Climate Network, a subset of the COOP data network. For each station, cold seasons
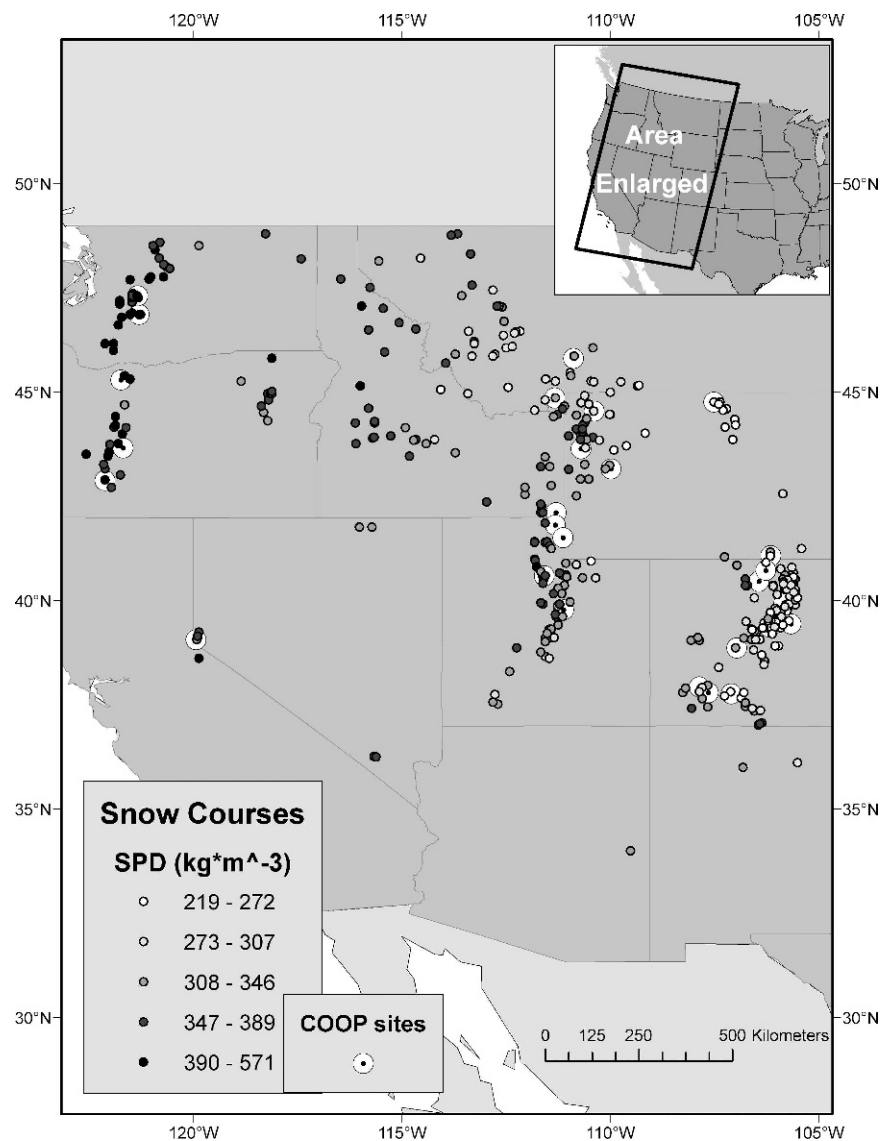
FIGURE 1. Snow courses (shaded dots indicating average April 1 *SPD* in kg m^{-3}) and COOP sites (white circle with center dot) with 15 or more years of quality-controlled data. All COOP sites shown here are within 50 m of elevation and 0.5° latitude and longitude of a snow course. All sites depicted were used in the composite analysis described in the methods section.

(November–March) that had more than 6.5% missing data for any weather element (maximum temperature, minimum temperature, precipitation, and snowfall depth) were eliminated from further analysis. Weather observers occasionally report the liquid equivalent of snowfall as exactly one-tenth of the daily measured snowfall (Knowles et al., 2006). Therefore, similar to Knowles et al. (2006), for each COOP station, the individual cold seasons with greater than 2% of the daily observations recording a snowfall to precipitation ratio of exactly 10 were discarded from the data set.

As mentioned above, four variables that control spring snowpack density are precipitation total, precipitation type, air temperature, and initial snowfall density (Brown et al., 2003; Kelly et al., 2003; Mizukami and Perica, 2008). These can be estimated for the winter season (November–March) antecedent to the April 1 *SPD* observations at each snow course site from the adjacent COOP sites (within 50 m in elevation and 0.5° latitude and longitude). Daily snowfall density was determined at each COOP site by use of the snow ratio, which is the depth of snowfall divided by the liquid equivalent (given that these values are in the same units). The snowfall density was then determined through Equation 1 above. Numerous previous studies have utilized the snow ratio to estimate snowfall density (Judson and Doesken, 2000; Roebber et al., 2003; Baxter et al., 2005; Ware et al., 2006;

Byun et al., 2008). Complications arise, however, when one uses COOP data to determine the snow ratio. These complications are well documented by Baxter et al. (2005) and include overestimation of the snow ratio due to precipitation gauge undercatch and underestimation due to mixed precipitation type. Despite these complications with snow ratios, Baxter et al. (2005) found considerable agreement with COOP–derived densities and those from more controlled studies. Baxter et al. (2005) tentatively attributed this to the canceling out of the mechanisms that are sources for inaccuracies for COOP derived densities.

In accordance with the standards set by Roebber et al. (2003) and used by previous studies (Baxter et al., 2005; Ware et al., 2006), daily snowfall density was only determined for days in which total precipitation was greater than 2.8 mm and total snowfall was greater than 50.8 mm. In addition, snowfall density was only determined for days in which the average temperature was below 0 °C and the maximum temperature did not exceed 4 °C. This additional constraint was applied to avoid calculating snow density during days with substantial liquid precipitation and for each station this constraint typically resulted in the exclusion of less than 5% of days that recorded snowfall. The average daily snowfall density (*SFD*) was then calculated for each winter.

TABLE 1

Descriptions of all variables used for regression analyses. The variable acronyms are used throughout the text.

	Variable	Acronym	Description	Source
Dependent Variable	Snowpack density	SPD	The spring (generally April 1) snowpack density	NRCS snow courses (or B03 model)
Independent Variable	Total winter precipitation	P	The total precipitation accumulated during a winter season (generally Nov–Mar)	COOP stations (or B03 model)
Independent Variable	Fraction of precipitation falling as snow	SFE/P	The total snowfall liquid equivalent (SFE) over P for a given winter season	COOP stations (or B03 model)
Independent Variable	Air temperature	T	Average daily temperature on days with no snowfall for a given winter	COOP stations (or B03 model)
Independent Variable	Snowfall density	SFD	Average density of freshly fallen snow for a given winter	COOP stations (or B03 model)

NRCS = U.S. Department of Agriculture National Resources Conservation Service.
B03 = Brown et al. (2003).
COOP = National Weather Service Cooperative Observer Network.

At each COOP station, the total precipitation (P) was calculated for each winter. To quantify the general form of precipitation recorded at a given COOP station over the course of winter, the author calculated the snowfall liquid equivalent (SFE) to precipitation ratio as used by Knowles et al. (2006) regarding trends in precipitation form in response to regional warming. For each winter, the total precipitation on days that recorded snowfall was calculated to estimate total SFE. The fraction of P that occurred as snowfall (SFE/P) was also determined. Lastly, the average daily temperature (T) for days that recorded no snowfall was calculated for each winter. This was used to estimate the air temperature over the existing snowpack for days that rapid densification due to snowmelt could possibly occur. It should be noted that wind was not considered as a predictor in this investigation because of the high likelihood of differing wind characteristics between snow courses and adjacent COOP sited due to the location-specific nature of wind in mountainous terrain.

To determine the importance of T, P, SFE/P, and SFD on April 1 SPD (see Table 1 for acronym descriptions) for the entire west the author standardized these variables for each COOP site and snow course site with 15 or more years of quality-controlled data (Fig. 1). Simple linear regression and stepwise regression ($\alpha <$ 0.05 to enter and $\alpha <$ 0.10 to remain in the model) were then performed on these yearly observations with the areal average of the standardized T, P, SFE/P, and SFD as the independent variables and the areal average of the standardized April 1 SPD as the dependent variable. It is important to note that for each winter, the observations were the composite of more than one-third (one-fifth) of the COOP stations (snow courses) with at least one COOP station and snow course south of 38°N, north of 38°N but south of 45°N, and north of 45°N. These subjective criteria were chosen to help ensure that each observation was representative of the entire western U.S.A. To explore the difference of this areal composite regression analysis between warm and cold locations, the author repeated the above process for four subgroups of the data sites in Figure 1. The subgroups were the COOP sites (and the adjacent snow courses) with average SFE/P (T) greater than 0.75 (-2.00 °C) and less than 0.75 (-2.00 °C). The boundary values of 0.75 and -2.00 °C were based on obvious breaks near the lower quartile of average SFE/P (T) by COOP site.

In order to identify spatial patterns in the controls of SPD, 24 snow courses were analyzed individually through linear regression (Table 2, Fig. 2). Fourteen of these stations were chosen for analysis based on their periods of record which yielded at least 25 years of data that coincided with quality controlled data at the adjacent COOP sites. The remaining 10 stations (with at least 13 years of data) were chosen to supplement the spatial coverage provided by the 14 stations with longer records. Greater than 10% of the April 1 snow depth observations at the Arizona snow course (Table 2) were zero; therefore, the data for the regression analysis in Arizona pertain to March 1 SPD and a winter season defined as November through February. Observations in the linear model for each snow course consisted of April 1 SPD as the dependent variable and the average of T, P, SFE/P, and SFD from adjacent COOP stations as the predictor variables (see Table 1 for variable descriptions).

For all regression analyses in this study, error normality and constant error variance were assessed through Lilliefors test for normality (Steinskog et al., 2007) and the Breusch-Pagan test (Rackauskas and Zuokas, 2007). If either of these assumptions critical for meaningful linear regression appeared to be invalid at the 0.05 level, Box-Cox transformations were preformed to help alleviate these issues (Box and Cox, 1964; Table 2). The appropriateness of a first-order linear model was qualitatively confirmed through the analysis of various scatter plots (not shown).

The empirical statistical relationships from the COOP and snow course data were compared to a simple snowpack model employed operationally by the Canadian Meteorological Centre and used to generate large-scale snow cover information to evaluate general circulation model snow cover output for the Atmospheric Model Intercomparison Project II (Brown et al., 2003). The model, detailed in Brown et al. (2003) (hereafter B03), is based on empirical equations and can be operated at fine horizontal and temporal resolutions with minimal computational resources. For this investigation, NARR 3-hourly 2 m air temperature and accumulated precipitation were used as inputs. From 1979 to 2009, simulations were conducted for each of the 4602 NARR grids located south of 49.0°N, north of 31.0°N, west of 102.5°W, and east of 130.0°W (a subjective bounding area for the western U.S.A.).

The B03 model reproduces SWE reasonably well. For the 12 snow courses that were within 5 km of a NARR grid, the median least squares slope was 1.318 and the median correlation was 0.628 (the median degrees of freedom was 26) with modeled April 1 SWE as a predictor of observed April 1 SWE. One should not expect perfect correlation (as well as slopes of exactly one) between the B03 model output and the nearby snow courses because considerable changes in snow characteristics can occur over small distances in mountainous terrain and manual snow course

B. M. SVOMA / 121

TABLE 2

The 24 snow course sites (bold) and the nearby COOP sites used in the individual regression analysis. Individual groupings of adjacent sites are delineated by row shading. Snow courses where error normality and constant error-variance issues were successfully alleviated by Box-Cox transformations are indicated by *. Snow courses for which Box-Cox transformations proved unsuccessful at alleviating these issues are indicated by **. OR—Oregon, ID—Idaho, MT—Montana, WY—Wyoming, CO—Colorado.

Station Name	Elev (m)	Lat. (°N)	Long. (°W)	State
North Umpqua **	**1298**	**43.27**	**122.15**	**OR**
Lemolo Lake 3 NNW	1254	43.35	122.21	OR
Wickiup Dam	1341	43.67	121.68	OR
Caldwell Ranch *	**1354**	**43.77**	**121.80**	**OR**
Wickiup Dam	1341	43.67	121.68	OR
Willow Flat	**1868**	**42.12**	**111.62**	**ID**
Bern	1835	42.33	111.38	ID
Lifton Pumping ST	1823	42.12	111.30	ID
Montpelier RS	1833	42.32	111.3	ID
Pierce RS	**948**	**46.50**	**115.80**	**ID**
Elk River 1 S	898	46.77	116.17	ID
Headquarters	982	46.62	115.80	ID
Nez Pierce	997	46.23	116.23	ID
Hebgen Dam *	**2015**	**44.87**	**111.32**	**MT**
Big Sky 2WNW	2028	45.10	111.32	MT
Hebgen Dam	1997	44.87	111.33	MT
Bryan Flat *	**1975**	**43.47**	**110.62**	**WY**
Alta 1 NNW	1981	43.77	111.03	WY
Bedford 3 SE	1977	42.87	110.90	WY
Bedford 2 SE	1949	42.87	110.90	WY
Moose	1991	43.65	110.70	WY
Aster Creek	**2385**	**44.27**	**110.62**	**WY**
Lake Camp *	**2394**	**44.55**	**110.40**	**WY**
Lewis Lake Divide	**2415**	**44.20**	**110.67**	**WY**
Thumb Divide	**2455**	**44.37**	**110.57**	**WY**
Lake Yellowstone	2422	44.55	110.38	WY
Telluride	**2708**	**37.91**	**107.80**	**CO**
Telluride 4WNW	2668	37.93	107.87	CO
Ames	2676	37.87	107.88	CO
Lake City	2667	38.02	107.30	CO
Rico	2708	37.70	108.03	CO
Baltimore	**2708**	**39.90**	**105.57**	**CO**
Grand Lake 1 NW	2683	40.27	105.81	CO
Grant	2669	39.45	105.67	CO
Crested Butte	**2745**	**38.86**	**107.00**	**CO**
Crested Butte	2725	38.87	106.97	CO
Glen Mar Ranch *	**2692**	**39.82**	**106.05**	**CO**
Grand Lake 1 NW	2683	40.27	105.81	CO
Grant	2669	39.45	105.67	CO
Redcliff	2651	39.52	106.37	CO
Middle Fork CG *	**2769**	**39.77**	**106.02**	**CO**
Dillon	2789	39.62	106.03	CO
Nast Lake **	**2677**	**39.30**	**106.60**	**CO**
Crested Butte	2725	38.87	106.97	CO
Redcliff	2651	39.52	106.37	CO
Silver Lake-Brighton	**2685**	**40.60**	**111.57**	**UT**
Brighton Cabin	**2677**	**40.60**	**111.57**	**UT**
ALTA	2686	40.58	111.63	UT
Silver Lake Brighton	2689	40.60	111.58	UT
East Portal	**2326**	**40.17**	**111.17**	**UT**
Scofield Dam	2348	39.78	111.12	UT
Soldier Summit	2298	39.92	111.07	UT
Tony Grove RS *	**1923**	**41.87**	**111.57**	**UT**
Randolph	1929	41.65	111.18	UT
Woodruff	1943	41.51	111.13	UT
Little Valley *	**1938**	**39.25**	**119.87**	**NV**
Glenbrook	1954	39.07	119.93	NV
Stateline-Harrah's	1922	38.97	119.85	NV

TABLE 2

Continued.

| Station Name	Elev (m)	Lat. (°N)	Long. (°W)	State
Virginia City	1950	39.30	119.63	NV
Bumping Lake *	**1062**	**46.87**	**121.30**	**WA**
Bumping Lake	1059	46.87	121.30	WA
Parkway 6 S	1093	46.92	121.53	WA
Tunnel Avenue	**754**	**47.32**	**121.35**	**WA**
Lake Keechelus	763	47.32	121.33	WA
Mormon Mountain	**2308**	**34.92**	**111.52**	**AZ**
Ft Valley	2260	35.27	111.73	AZ
Happy Jack RS	2301	34.73	111.4	AZ

observations are frequently recorded within several days of April 1 (not always on April 1 exactly). Regression analyses as detailed above were applied to each grid that had no less than 27 (out of 30; 1980–2009) non-zero April 1 snow depths. The dependent and independent variables were derived from the model and are detailed in Table 1.

Results

The density of the spring snowpack across the western U.S.A. displays a west-to-east gradient with denser snow packs near the coast (Fig. 1). This is consistent with descriptions of snow pack characteristics by previous avalanche studies (e.g., Mock, 1995; Mock and Birkeland, 2000) and Mizukami and Perica (2008), who suggested that coastal areas with abundant heavy snowfall tend to have higher density snow cover. Analyses of scatter plots for the 19 areal composited yearly observations (Fig. 3) indicate that cold season P had the most apparent relationship with April 1 SPD. A slight positive relationship may also exist between SFD and SPD (Fig. 3). Interestingly, no relationship is evident between SFE/P and SPD (or T and SPD). This is likely due to the relatively high elevations of many stations used in this study. The winter temperatures at most of the locations examined in this study were generally cold enough such that rain events and significant melt events were rare as suggested by a median average SFE/P of 0.95 and a median average T of -5.96 °C. One should not expect these isolated densification and ablation events to greatly influence SPD considering the more significant influences of other variables such as P.

As suggested by the scatter plots (Fig. 3), simple linear regression results indicate that P had the greatest impact on SPD over the western U.S.A. as a whole. The composite regression analysis with the standardized west-wide averages displays a highly significant ($p = 0.0051$, $R^2 = 0.3775$) positive relationship between P and April 1 SPD. Winter T, SFE/P, and SFD all explained an insignificant amount of variance in April 1 SPD. Furthermore, stepwise regression yielded a regression model with only P as a predictor variable for SPD. The significant positive relationship between P and SPD is likely due to two reasons. First, initial snowfall densification due to compaction at the surface (Judson and Doesken, 2000; Byun et al., 2008) is likely enhanced during years that receive high precipitation due to potentially higher snowfall rates. Second, the presence of more SWE likely increases densification rates from gravitational compaction throughout the winter (Mizukami and Perica, 2008).

At the 24 snow courses analyzed individually through regression analysis there was no evidence of any relationship between SFD and April 1 SPD. Therefore, the positive relation-
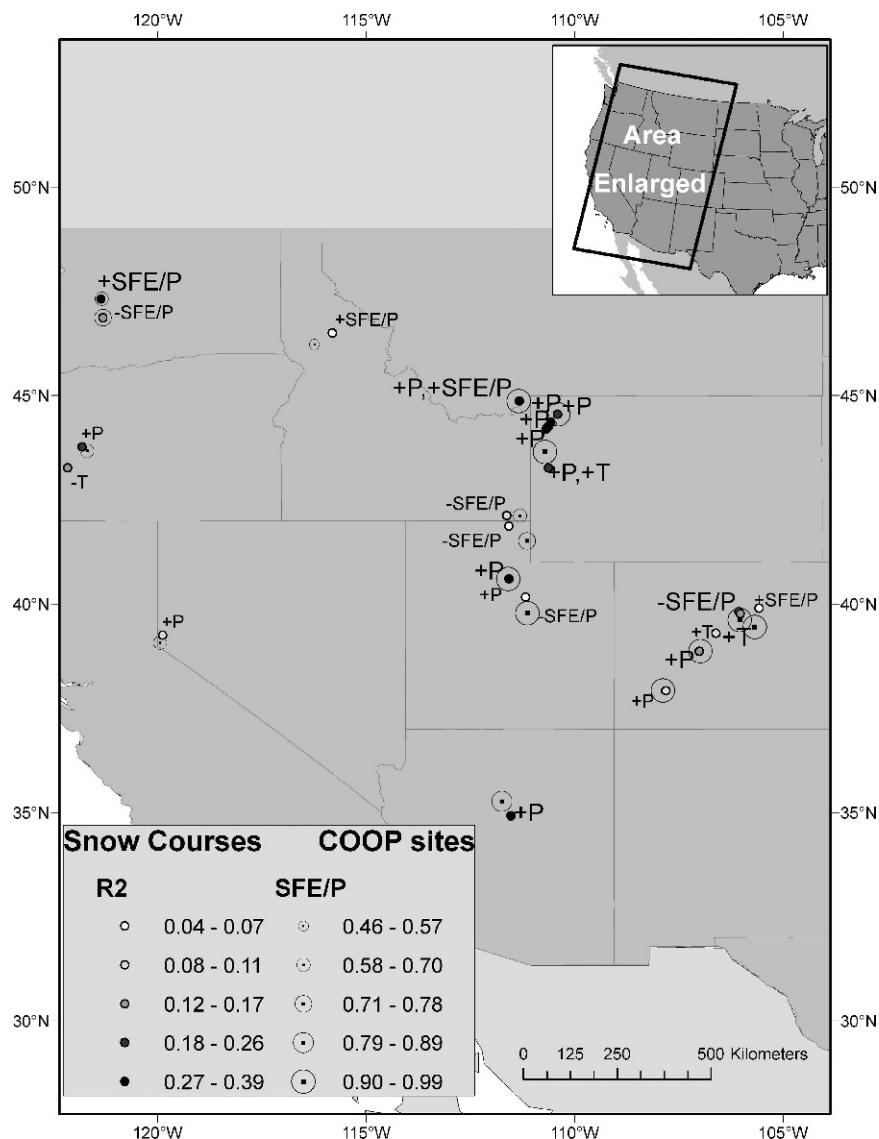
FIGURE 2. The 24 snow courses (dots; darker shading corresponds to higher R^2) used for individual regression analysis. The COOP sites (circled dots; larger circles equal higher average SFE/P) represent the location of the COOP sites with the most years of data in common with the adjacent snow course. The winter season variable (see Table 1 for acronym descriptions) that explained the most variance in April 1 SPD from simple linear regression is displayed next to each snow course (followed by other significant variables ($p < 0.10$) that remained in the stepwise regression model). Predictors significant with 95% confidence are in larger font. The R^2 values are with respect to the first step of stepwise regression. The direction of linear relationship is indicated (+ = positive, − = negative), and locations with regression results from transformed data are indicated in Table 2.

ship between P and April 1 SPD (Fig. 3) may be best explained by increased gravitational compaction due to greater SWE, as the variability in SFD should mirror the variability in the initial densification from surface compaction. The positive relationship between P and SPD appears weakest in warmer regions which are indicated by low values of SFE/P (Fig. 2; it should be noted that the values of SFE/P represent the weighted average [weighted by the number of years with valid data] of all COOP sites adjacent to
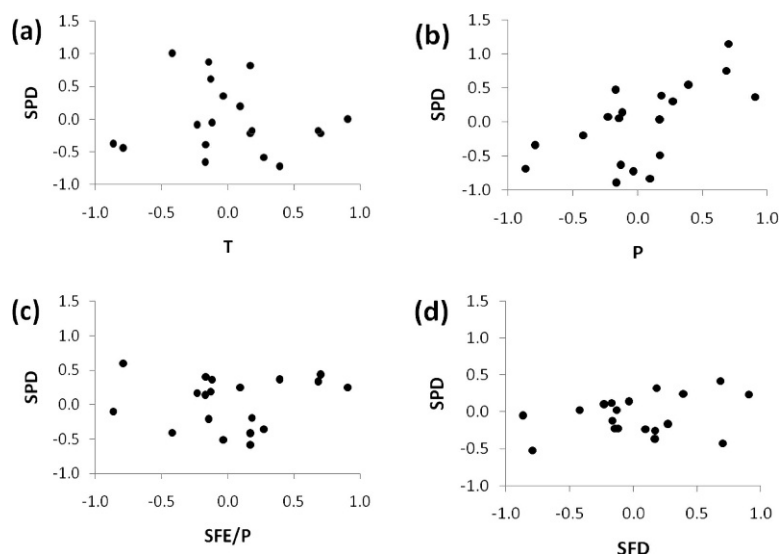
FIGURE 3. Scatter plots of the standardized composite April 1 SPD (snowpack density) versus Nov–Mar. (a) T (mean air temperature), (b) P (total precipitation), (c) SFE/P (fraction of precipitation fall as snow), and (d) SFD (mean snowfall density). See Table 1 for a more detailed explanation of these variables. Each observation represents the average over the station network (Fig. 1) for a given year.

B. M. SVOMA / 123
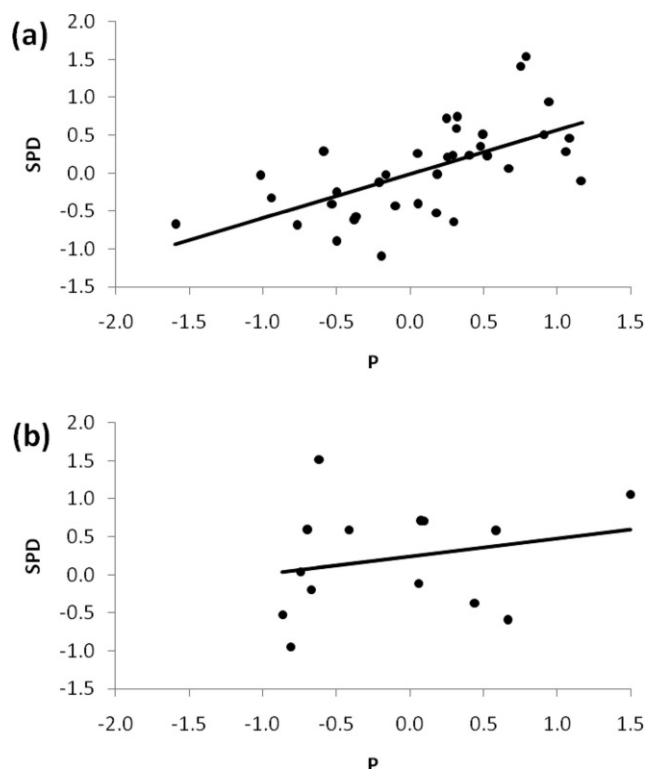
FIGURE 4. Scatter plots and simple linear regression fits (black line) of the standardized composite April 1 *SPD* versus Nov–Mar *P* for (a) stations with average *SFE/P* > 0.75 and (b) stations with average *SFE/P* < 0.75. Each observation represents the average over the station network for a given year.

a given snow course). In contrast, significant positive relationships between *P* and *SPD* are only seen in the higher elevation interior mountains, which are typically colder with high values of *SFE/P* (Fig. 2). The more numerous rain events and/or melt events in the warmer coastal or low-elevation regions likely impart a greater influence (relative to the colder interior mountains) on April 1 *SPD*. Rain and snowmelt ablate snow cover and therefore may weaken the influence of *P* on *SPD* by reducing *SWE* and lessening the effects of gravitational compaction. In addition, rain and snowmelt can increase snowpack density through refreezing in pore space while heavy rainfall can decrease density through abolishing the structure of the snowpack such that water can no longer be efficiently retained by the snow. This would act as a further source of noise for the identification of a statistical relationship between *P* and *SPD*.

Further evidence of this modulation of the influence of *P* on April 1 *SPD* can be seen in Figure 4. The slope of the simple linear fit (Fig. 4) for locations with average *SFE/P* greater than 0.75 (0.580, $p < 0.001$; Fig. 4a) is larger than locations with average *SFE/P* less than 0.75 (0.232, $p = 0.423$; Fig. 4b). Similarly, the slope of the simple linear fit for locations with average *T* lesser than -2.00 °C locations (0.638, $p < 0.001$) is larger than locations with average *T* greater than -2.00 °C (0.387, $p = 0.246$).

As with the empirical data, B03 model results indicate that *P* is the most important predictor of April 1 *SPD* over the western U.S.A. Out of the 113 NARR grid locations analyzed through simple linear regression, *P* was the most significant single predictor for 54 locations and the relationships between *P* and April 1 *SPD* were overwhelmingly positive as expected (50 had positive slopes, 31 of which were significant at the 0.05 level). For the other 59 locations, none of the remaining three variables stood out as more important than the others with *SFE/P* as the most significant single predictor for 23 locations, and *T* and *SFD* as the most significant predictor for 18 locations each.

From the B03 model, the regions of the western U.S.A. displaying the most coherent relationship between *P* and April 1 *SPD* (Fig. 5) are largely the same as the empirical analysis (Fig. 2). April 1 *SPD* is highly positively correlated to *P* in northwest Wyoming (Fig. 2 and Fig. 5), a region of high elevation and cold temperature. Similar to the empirical results (Fig. 2) for the B03 model, April 1 *SPD* is more correlated with *SFE/P* than *P* in the Pacific Northwest (Fig. 5), a region of lower elevations and warmer temperatures relative to the interior mountains. The more widespread coverage (relative to the snow course coverage) of the B03 model simulations reveals other high-elevation/cold regions that display the obvious positive relationship between *P* and April 1 *SPD*, such as the northern Rockies in Montana and the high elevations of the Sierra Nevada in California. An obvious difference between the B03 model results and the empirical results is the region of significant positive relationships between *SFD* and April 1 *SPD*, adjacent to the region dominated by significant relationships between *P* and April 1 *SPD* in northwest Wyoming. Empirically, there was no evidence of a relationship between *SFD* and April 1 *SPD*. It is beyond the scope of this paper to explore this difference in further detail; however, this may be attributed to the methodological differences in calculating the model *SFD* (from the Hedstrom and Pomeroy equation [Brown et al., 2003]) and the empirical *SFD* (from daily COOP snow ratios).

Summary and Conclusions

Knowledge of spring snowpack density benefits the scientific communities concerned with wet avalanche forecasting, climate modeling, and snow cover modeling. In this study, four variables were statistically related through linear regression to spring *SPD*. These variables were (1) average air temperature (on days with no snowfall), (2) average snowfall density, (3) the fraction of precipitation falling as snow, and (4) total precipitation. These variables characterized the antecedent winter conditions contributing to the build up of spring snowpack.

Through linear regression, total precipitation was the most significantly ($r = +0.614$, $p = 0.0051$) related to spring snowpack density. The importance of precipitation is likely due to the relatively cold winter climates of the sites examined. Over the entire COOP network the median average winter *SFE/P* was 0.95, thus generally limiting the influence that mixed precipitation types could have on snowpack density. Similarly, air temperatures were generally well below 0 °C, thus limiting densification due to snowmelt. However, variability in the strength of the relationship between *P* and April 1 *SPD* over the western U.S.A. appeared to be influenced by temperature. Regions with lower values of *SFE/P*, typically near the coast and in lower elevations, showed much weaker relationship between *P* and *SPD* than regions with colder temperatures and higher values of *SFE/P*. Areal composited regression analyses for locations with winter *SFE/P* less than 0.75 displayed an insignificant positive coefficient when standardized *P* was regressed against standardized April 1 *SPD*. This slope was nearly half that of the highly significant ($p < 0.001$) slope from the regression line for areas with average winter *SFE/P* greater than 0.75. A nearly identical pattern resulted from composite regression analyses when the network was divided based on *T*, with *SPD* in warmer locations (>-2.00 °C) displaying weaker relationship with *P* than at colder locations. These empirical results (i.e., a positive
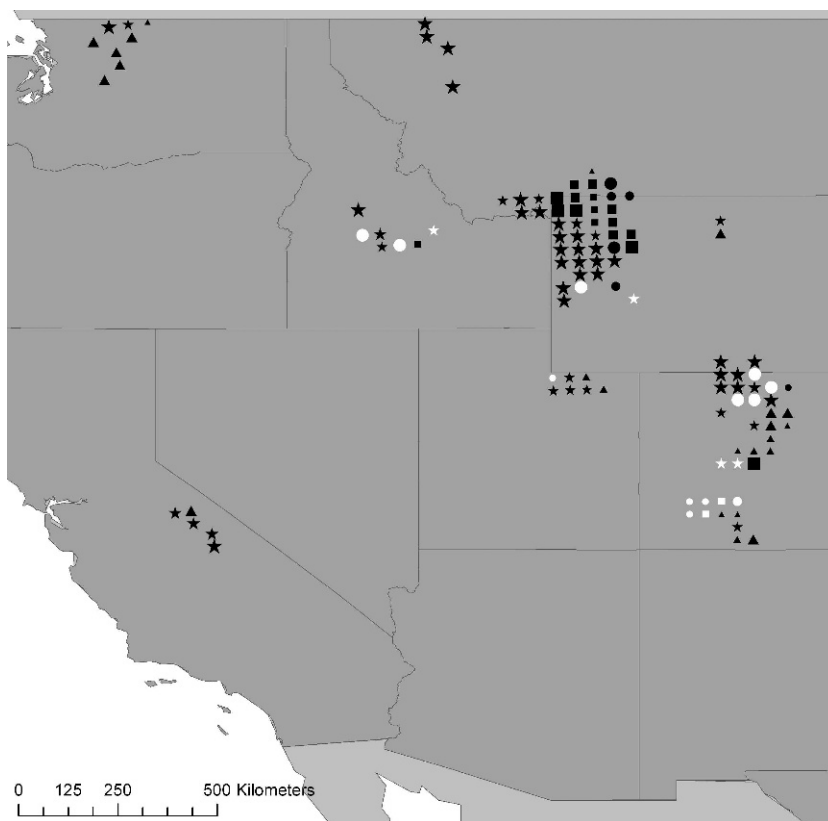
FIGURE 5. The most significant single predictors of April 1 *SPD* as determined from the Brown et al. (2003) simple snowpack model for NARR grids that had no less than 27 (out of 30; 1980–2009) non-zero April 1 snow depths. Positive (negative) slopes are indicated by black (white) symbols. The largest symbols indicate that the predictor is significant at the 0.05 level, medium symbols indicate that the predictor is significant at the 0.10 level, and the smallest symbols indicate that the predictor is not significant at the 0.10 level. *P* is represented by stars, *T* by circles, *SFE/P* by triangles, and *SFD* by squares. Predictor variable acronyms are described in Table 1.

relationship between *P* and spring *SPD* over the western U.S.A. overall, but mainly confined to high elevation/cold regions), were supported by a simple snowpack model.

Increasing spring snowpack density with winter precipitation (or snowfall in particular) is likely due to (1) higher densification rates throughout winter due to increased gravitational compaction from more *SWE* (Mizukami and Perica, 2008) and/or (2) higher initial snowfall densities due to rapid compaction at the surface from higher precipitation rates which may be associated with wetter winters (Judson and Doesken, 2000; Byun et al., 2008). However, compaction from greater *SWE* seems a more likely cause due to the lack any significant relationship between *P* and *SFD*, as the variability in *SFD* should mirror the variability in the initial densification from surface compaction.

The significance of this study is twofold. First, the positive relationship between spring *SPD* and winter snowfall totals suggests that warm spring seasons following wet winters are optimal conditions for wet avalanches, which occur most frequently when air temperatures rise above 0 °C over snow cover that has low cohesion due to high water content (e.g., density; Roeger et al., 2001). Second, establishing the response of spring snowpack density to antecedent winter conditions, shown here to agree with theory and to be reproducible by a simple snowpack model, contributes to a slim body of empirical literature within a realm of climate science concerned with modeling snow cover for a region that is heavily dependent on snowfall for a sustainable water supply.

Acknowledgment

References Cited

Balk, B., and Elder, K., 2000: Combining binary decision tree and geostatistical methods to estimate snow distribution in a mountain watershed. *Water Resources Research*, 36: 13–26.

Baxter, M. A., Graves, C. E., and Moore, J. T., 2005: A climatology of snow-to-liquid ratio for the contiguous United States. *Weather and Forecasting*, 20: 729–744.

Bossolasco, M., 1954: Newly fallen snow and air temperature. *Nature*, 174: 362–363.

Box, G. E. P., and Cox, D. R., 1964: An analysis of transformations. *Journal of the Royal Statistical Society Series B–Statistical Methodology*, 26: 211–252.

Brown, R. D., 2000: Northern hemisphere snow cover variability and change, 1915–97. *Journal of Climate*, 13: 2339–2355.

Brown, R. D., Brasnett, B., and Robinson, D., 2003: Gridded North American monthly snow depth and snow water equivalent for GCM evaluation. *Atmosphere–Ocean*, 41: 1–14.

Byun, K. Y., Yang, J., and Lee, T. Y., 2008: A snow-ratio equation and its application to numerical snowfall prediction. *Weather and Forecasting*, 23: 644–658.

Colbeck, S. C., 1982: An overview of seasonal snow metamorphism. *Reviews of Geophysics*, 20: 45–61.

Diamond, M., and Lowry, W. P., 1954: Correlation of density of new snow with 700-millibar temperature. *Journal of Meteorology*, 11: 512–513.

Elder, K., Rosenthal, W., and Davis, R. E., 1998: Estimating the spatial distribution of snow water equivalence in a montane watershed. *Hydrological Processes*, 12: 1793–1808.

Erxleben, J., Elder, K., and Davis, R., 2002: Comparison of spatial interpolation methods for estimating snow distribution in the Colorado Rocky Mountains. *Hydrological Processes*. doi:10.1002/hyp.1239.

Flanner, M. G., and Zender, C. S., 2006: Linking snowpack microphysics and albedo evolution. *Journal of Geophysical Research–Atmospheres*. doi:10.1029/2005jd006834.

Garen, D. C., and Marks, D., 2005: Spatially distributed energy balance snowmelt modelling in a mountainous river basin: estimation of meteorological inputs and verification of model results. *Journal of Hydrology*, 315: 126–153.

Hedstrom, N. R., and Pomeroy, J. W., 1998: Measurements and modelling of snow interception in the boreal forest. *Hydrological Processes*, 12: 1611–1625.

Judson, A., and Doesken, N., 2000: Density of freshly fallen snow in the Central Rocky Mountains. *Bulletin of the American Meteorological Society*, 81: 1577–1587.

Kaempfer, T. U., and Schneebeli, M., 2007: Observation of isothermal metamorphism of new snow and interpretation as a sintering process. *Journal of Geophysical Research–Atmospheres*. doi:10.1029/2007jd009047.

Kelly, R. E., Chang, A. T., Tsang, L., and Foster, J. L., 2003: A prototype AMSR-E global snow area and snow depth algorithm. *IEEE Transactions on Geoscience and Remote Sensing*, 41: 230–242.

Knowles, N., Dettinger, M. D., and Cayan, D. R., 2006: Trends in snowfall versus rainfall in the Western United States. *Journal of Climate*, 19: 4545–4559.

Lazar, B., and Williams, M., 2008: Climate change in western ski areas: potential changes in the timing of wet avalanches and snow quality for the Aspen ski area in the years 2030 and 2100. *Cold Regions Science and Technology*, 51: 219–228.

Maeno, N., and Ebinuma, T., 1983: Pressure sintering of ice and its implication to the densification of snow at polar glaciers and ice sheets. *Journal of Physical Chemistry*, 87: 4103–4110.

Meloysund, V., Leira, B., Hoiseth, K. V., and Liso, K. R., 2007: Predicting snow density using meteorological data. *Meteorological Applications*, 14: 413–423.

Mizukami, N., and Perica, S., 2008: Spatiotemporal characteristics of snowpack density in the mountainous regions of the western United States. *Journal of Hydrometeorology*, 9: 1416–1426.

Mock, C. J., 1995: Avalanche climatology of the continental zone in the Southern Rocky Mountains. *Physical Geography*, 16: 165–187.

Mock, C. J., and Birkeland, K. W., 2000: Snow avalanche climatology of the western United States mountain ranges. *Bulletin of the American Meteorological Society*, 81: 2367–2392.

Mote, P. W., Hamlet, A. F., Clark, M. P., and Lettenmaier, D. P., 2005: Declining mountain snowpack in western North America. *Bulletin of the American Meteorological Society*, 86: 39–49.

Pierce, D. W., Barnett, T. P., Hidalgo, H. G., Das, T., Bonfils, C., Santer, B. D., Bala, G., Dettinger, M. D., Cayan, D. R., Mirin, A., Wood, A. W., and Nozawa, T., 2008: Attribution of declining western US snowpack to human effects. *Journal of Climate*, 21: 6425–6444.

Power, B. A., Summers, P. W., and Davignon, J., 1964: Snow crystal forms and riming effects as related to snowfall density and generally storm conditions. *Journal of the Atmospheric Sciences*, 21: 300–305.

Rackauskas, A., and Zuokas, D., 2007: New tests of heteroskedasticity in linear regression model. *Lithuanian Mathematical Journal*, 47: 248–265.

Roebber, P. J., Bruening, S. L., Schultz, D. M., and Cortinas, J. V., 2003: Improving snowfall forecasting by diagnosing snow density. *Weather and Forecasting*, 18: 264–287.

Roeger, C., McClung, D., Stull, R., Hacker, J., and Modzelewski, H., 2001: A verification of numerical weather forecasts for avalanche prediction. *Cold Regions Science and Technology*, 32: 189–205.

Steinskog, D. J., Tjostheim, D. B., and Kvamsto, N. G., 2007: A cautionary note on the use of the Kolmogorov-Smirnov test for normality. *Monthly Weather Review*, 135: 1151–1157.

Sturm, M., and Benson, C. S., 1997: Vapor transport, grain growth and depth-hoar development in the subarctic snow. *Journal of Glaciology*, 43(143): 42–59.

Sturm, M., McFadden, J. P., Liston, G. E., Chapin, F. S., Racine, C. H., and Holmgren, J., 2001: Snow-shrub interactions in Arctic tundra: a hypothesis with climatic implications. *Journal of Climate*, 14(3): 336–344.

Ware, E. C., Schultz, D. M., Brooks, H. E., Roebber, P. J., and Bruening, S. L., 2006: Improving snowfall forecasting by accounting for the climatological variability of snow density. *Weather and Forecasting*, 21: 94–103.